International Journal of Thermophysics, Vol. 15, No. 6, 1994

Simulation of a Liquid–Liquid Floating Interface[1]

J. Stecki[2]

The planar interface between two simple liquids interacting with 6–12 LJ potentials was simulated by molecular dynamics at a low temperature. The peculiar physical picture, the new "breathing" mode, the 2×2 matrix of the structure factors $S(k_\perp)$, and the interfacial dynamic structure factor $S(k, \omega)$, are reported.

KEY WORDS: breathing mode; floating interface; Goldstone mode; miscibility gap; simple liquids; structure factor.

1. INTRODUCTION

Simulations of liquid–liquid interfaces in the literature have not been very numerous [1]. Our work has been motivated by the following considerations. First, creating and maintaining a (planar) stable interface separating two immiscible simple liquids is easy compared with a single-component liquid–vapor system and there is a better chance of obtaining quantitative information. At the level of one-particle functions there is little to add to the existing body of knowledge [2, 3], though elsewhere [4] we are addressing the issue of density oscillations in the static equilibrium density profiles. See Ref. 5 for a different context. At the level of the two-point functions such as the density–density correlation function (DDCF), little is known in $d = 3$ beyond the (asymptotic) results of the standard capillary-wave (CW) theory [2, 3], whereas considerable progress has been made in $d = 2$ for models such as the solid-on-solid (SOS) model by both the numerical transfer matrix and the analytical calculations [6–9]. In fact the DDCF and the direct correlation function $C(\mathbf{r}_1, \mathbf{r}_2)$ are both known. In $d = 3$ the shape of the DDCF or C in the inhomogeneous region known

[1] Paper presented at the Twelfth Symposium on Thermophysical Properties, June 19–24, 1994, Boulder, Colorado, U.S.A.

[2] Institute of Physical Chemistry, Polish Academy of Sciences, Department III, Kasprzaka 44/52, 01-224 Warsaw, Poland.

0195-928X/94/1100-1103$07.00/0

as "the interface" is not known even in qualitative terms; we expect to obtain some information. In particular, the widely used and very successful "density functional theory" relies on ad hoc approximations made at the level of the two-point functions; the best one can currently do is to enforce that C is equal everywhere to the (known) C_b of the bulk liquid. Thus the shapes of DDCF and of C in the interfacial zone are of interest.

Second, there is a great current interest in systems with a surfactant present, but interfaces in those systems will be understood, in particular in quantitative terms, by contrasting with the same system without surfactant.

Third, the dynamics of the interface has never been studied except for Ref. 1, where the self-diffusion coefficient has been determined. Although the "simulation window" in frequency ω and wave-vector $\mathbf{k}$ is limited, some information on the intermediate scattering function $I(k, t)$ can be obtained and even $S(k, \omega)$ sometimes may be calculated.

In this paper we report some of the results for the low-temperature regime. The latter ought to correspond perfectly with the usual assumptions of the CW theory.

In Section 2 we describe the simulation setup and the model system. In Section 3 we discuss the "breathing mode" which we have discovered in our system. In Section 4 we describe the matrix of static structure factors $S_{ij}(k)$ in the interfacial zone, and in Section 5 we show some results on the intermediate scattering function $I(k, t)$ and the dynamic structure factor $S(k, \omega)$.

2. THE SIMULATION SETUP AND THE INTERFACE

The rectangular volume periodic in all three directions $V = L_x \times L_y \times L_z$ with $L_x = L_y$ is filled with a rectangular slab of N_a particles of species "a" extending from $z = (1/4)L_z$ to $z = (3/4)L_z$ and an identical slab of N_b particles of species "b" extending from $z = (3/4)L_z$ to $z = (5/4)L_z$ equal modulo L_z to $z = (1/4)L_z$. We take $N_a = N_b$. The model particles interact with the Lennard–Jones (6–12) potential

$$u_{ss'}(r) = 4\varepsilon[(\sigma_{ss'}/r)^{12} - \alpha(\sigma_{ss'}/r)^6] \tag{1}$$

and we take $\sigma_{aa} = \sigma_{bb} = \sigma_{ab}$, $\alpha = 1$, and $\varepsilon_{aa} = \varepsilon_{bb}$. Thus particles "a" and "b" are identical. In this way we dispose of the unnecessary complications introduced by the difference in size or potential depth. For the u_{ab} potential we take $\alpha = 0$. Hence $\alpha = 1$ corresponds to the full attraction of the LJ (6–12) potential and $\alpha = 0$ corresponds to the *limiting case* of pure repulsion. A slab of bulk LJ liquid was duplicated and the two slabs were brought into contact; two planar interfaces near $z = L_z/4$ and near

$z = (3/4)L_z$ were thus created. Simulations have been performed for $N = N_a + N_b$ equal to 1024, 2048, 4096, and 9196. Results are reported here for the following data point: volume $V/\sigma^3 = 7.5 \times 7.5 \times 23.0$, number of particles $N = 512 + 512$, overall density $\rho\sigma^3 = 0.7915$, bulk density $\rho\sigma^3 = 0.8408$, temperature $kT/\varepsilon = 1.0$, normal pressure $p_{zz}\sigma^3/\varepsilon = 2.075$, surface tension $\gamma\sigma^2/\varepsilon = 3.039$, timestep $0.005\sigma(\varepsilon/\mathrm{m})^{1/2}$, length of typical run $\sim 0.5 \times 10^6$ timesteps, lowest k-vector $k\sigma = 0.83$, and typical box for $S(k)$ $v_\sigma = L_x \times L_y \times 1.4\sigma$. The unit of time is $\sigma(\varepsilon/m)^{1/2}$. The bulk phases were condensed liquids. The canonical MD simulations (NVT-MD) were performed as described in Ref. 10 with a Nose–Hoover thermostat [10] in all simulations except for the adiabatic run used for extraction of the intermediate scattering functions. The time-reversible energy- and momentum-conserving Verlet algorithm was used [10].

The microscopic structure of the interface turned out to be surprising at first. The two liquid slabs clearly separate in space, forming a "sheet of vaccum" in between. Not only the equilibrium total density goes through a minimum but also the individual density profiles are shifted away from each other. At the low $T = 1$, each bulk phase consists of almost pure "a" or "b", respectively, i.e., the solubility of a in b and conversely are much too low to be observed; it is then meaningful to introduce the two "kinks" $\zeta_a(x, y), \zeta_b(x, y)$ in terms of which the corresponding "number density operators," i.e., instantaneous microscopic number densities are defined for each instantaneous configuration

$$\rho_a(\mathbf{r}) = \rho_a^b \eta(z - \zeta_a(x, y)) \tag{2}$$

$$\rho_b(\mathbf{r}) = \rho_b^b \eta(-z + \zeta_b(x, y)) \tag{3}$$

We find there is *a gap between two kinks*,

$$\Delta(x, y) \equiv \zeta_b(x, y) - \zeta_a(x, y) \tag{4}$$

which *need not be constant*. Here $\eta(x) = 1$ if $x > 0$, $\eta(x) = 0$ if $x < 0$ is the Heaviside function. Δ is the local thickness of the *fluctuating sheet of vacuum*. At the state point reported here, $\langle \Delta \rangle$ was of the order of 0.8–1.1σ.

This picture can be understood as follows: Our two simple liquids separate for energetic reasons, i.e., because a–a or b–b interactions are more favorable than a–b interactions. Effectively, the two liquid slabs repel each other and would fly apart were it not for the geometry of the finite volume. The pressure p_{zz} is positive. These effects no doubt are emphasized by our choice of interactions but, I believe, are general.

3. DYNAMICS OF TWO LIQUID SLABS

At low temperatures and liquid densities, the two slabs of bulk liquids "a" and "b" are incompressible. The total linear momentum **P** is conserved by the MD algorithm, the total linear momentum $P_z^a(t)$, of "a" particles (all concentrated in the "a"-slab) need not be conserved. Only

$$P_z(t) = P_z^a(t) + P_z^b(t) = 0 \tag{5}$$

as we enforce $\mathbf{P} = 0$ at time $t = 0$. A typical plot of $\langle P_z^a(0)\, P_z^a(t)\rangle$ is shown in Fig. 1.

Clearly we see a separate oscillatory mode. In the continuum approximation (and assuming that bulk "a" contains no "b's" and conversely), the interaction of two slabs is

$$U_{ab} = \pi\rho_a\rho_b A[\Delta^{-8}/90 - \alpha\Delta^{-2}/3] \tag{6}$$

where $A = L_x L_y$ is the area and Δ is the distance (gap) between two slabs.

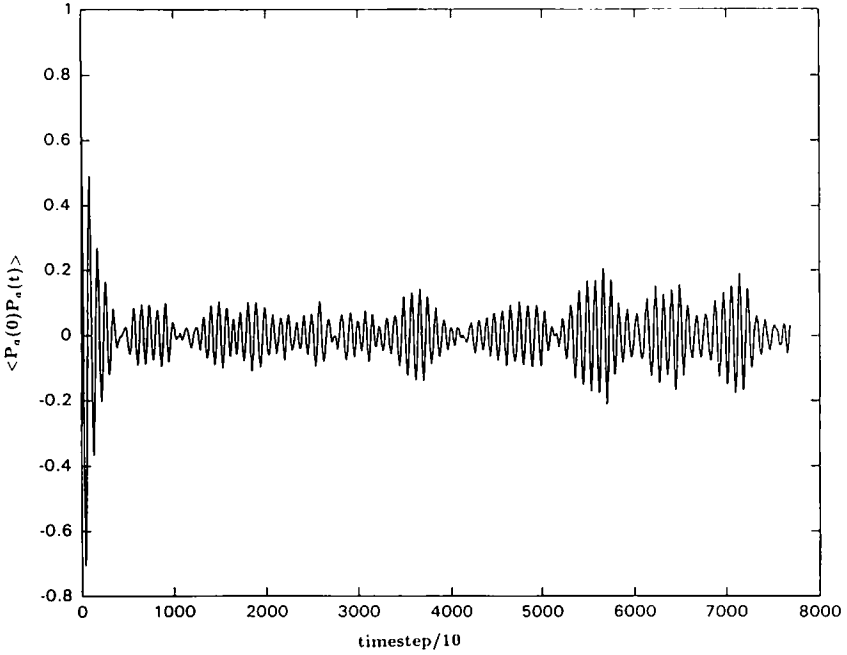

Fig. 1. Autocorrelation $\langle P_z^a(0)\, P_z^a(t)\rangle$. $P_z^a(t)$ is the total momentum of "a"-particles in the z direction. The x coordinate is (number of timesteps)/10.

For our choice $\alpha = 0$, U_{ab} is purely repulsive. Assuming the slabs incompressible, at equilibrium we have

$$p_{zz}A = -(dU_{ab}/d\Delta) \tag{7}$$

This determines Δ_0, the gap at static equilibrium. Assuming harmonic motion we calculate

$$(1/2)U'' = 36U_{ab}(\Delta_0)/\Delta_0^2 \tag{8}$$

and the circular frequency (for two identical slabs, putting mass $m = 1$) is given by

$$\omega^2 = \pi\rho_a^2 A(3.2/N_a)/\Delta_0^{10} \tag{9}$$

The equilibrium gap is controlled by the normal pressure p_{zz}; increasing the pressure by diminishing L_z (volume V at constant A) forces a decrease in Δ_0. For our data point, semiquantitative agreement is obtained with the aid of Eq. (9); $\omega = 1.32$ for $\Delta_0 = 0.909$ and $\omega = 1.49$ for $\Delta_0 = 0.887$ are predicted as against $\omega = 1.38$ determined from Fourier analysis of data shown in Fig. 1 (and of several other runs).

Clearly the mode we are describing is characteristic of an interface of a confined fluid and is in this sense a finite-size effect. It will be present in a variety of situations.

If the compressibility of the liquid slabs is not neglected, for two slabs separated by two gaps and joined by periodicity in the z-direction, the center-of-mass positions Z_1 and Z_2 must be now related by

$$Z_2 = Z_1 + l_1/2 + \Delta_1 + l_2/2 \tag{10}$$

with the constraint

$$l_1 + \Delta_1 + l_2 + \Delta_2 = L_z$$

Also, Eq. (6) is generalized to

$$U = U_a(V_1) + U_{ab}(\Delta_1) + U_b(V_2) + U_{ab}(\Delta_2) \tag{11}$$

where $V_1 = Al_1$, $V_2 = Al_2$. The second derivatives of U require now the compressibility of bulk liquids, but at these frequencies the static compressibility might better be replaced by the high-frequency bulk modulus. The dynamics is described by four coordinates Z_1, Z_2, Δ_1, and Δ_2 with one constraint and, in the harmonic approximation, by the 4×4 matrix of second derivatives of U. The theory of small vibrations [11] leads to a determinantal equation of the form $|X_{ij} - \omega^2 Y_{ij}| = 0$ with known elements

X_{ij} and Y_{ij} of matrices **X** and **Y**. $U_{ab}(A_i)$ is now also coupled to l_j through the $\rho_a\rho_b$ term. A thorough analysis of the resulting frequencies will be published elsewhere; so far from our calculations, only one frequency results. Simulation shows there is at least a second frequency.

Increasing N decreases ω; an increase in the surface area A due to capillary waves will complicate the simple notions outlined above, as the boundary of the slab will not be flat anymore.

4. STATIC STRUCTURE FACTORS

The static structure factor is [13]

$$S(k) = \langle \rho_{-\mathbf{k}} \rho_{\mathbf{k}} \rangle \tag{12}$$

where

$$\rho_{\mathbf{k}} = \sum_j e^{i\mathbf{k}\mathbf{r}_j}$$

is a Fourier component of the density $\rho(\mathbf{r})$. It is a well-known prediction of the CW theory that the DDCF's in the plane of the interface as $1/k^2$ in the absence of damping

$$\langle \tilde{\zeta}_{-\mathbf{k}} \tilde{\zeta}_{\mathbf{k}} \rangle \sim 1/(k^2 + D) \tag{13}$$

where $\tilde{\zeta}_{\mathbf{k}}$ is the well-known (Fourier-transformed) kink introduced in Section 2. In what follows **k** denotes the Fourier vector $\mathbf{k}_\perp \equiv (k_x, k_y)$. Within the kink approximation the density $\rho(z)$ by Eqs. (2) and (3); now we approximate well the l.h.s. of Eq. (13) by collecting averages $\langle \rho_{\mathbf{k}} \rho_{-\mathbf{k}} \rangle_\sigma$ in a volume "v_σ," which is a parallelepiped $L_x \times L_y \times (z_u - z_l)$ centered on the interface $\tilde{\zeta}_{k=0} = z_{00} \equiv (z_u + z_l)/2$. Now

$$\int_{z_u}^{z_l} dz_1 \int_{z_u}^{z_l} dz_2\, \rho(z_1; x_1, y_1)\, \rho(z_2; x_2, y_2)$$
$$= (\zeta(x_1, y_1) - z_l)(\zeta(x_2, y_2) - z_l) \times \text{const.} \tag{14}$$

and with translational invariance in the x and y directions, for $\mathbf{k} \neq 0$,

$$\langle \tilde{\zeta}_{-\mathbf{k}} \tilde{\zeta}_{\mathbf{k}} \rangle = \text{const.} \times \langle \rho_{\mathbf{k}} \rho_{-\mathbf{k}} \rangle_\sigma \tag{15}$$

For a low temperature, it is possible to define the kink for each microscopic configuration. One way of constructing the kink [1] consists of making a grid in the xy plane and finding in each square the particle with extremal z coordinate. The collection of these $z(x, y)$ coordinates may

then be used to construct smooth $\zeta_\gamma(x, y)$ surfaces. A better construction takes into account multiple values of height at a given point on the surface, in the form of overhangs or folds, and cavities. We introduce a fictitious particle which probes the shape of the surface but does not affect the real particles of the system. We assume a hard-sphere interaction, with collision diameter d in units of σ between the probe and the real particles; $d = 1/2$ corresponds to a point probe. Starting from $\mathbf{r} = (0, 0, z_{00})$, the probe attempts to penetrate without overlap into the bulk fluid on one side of the interface. The surface generated by the probe is a collection of spherical segments, each of radius d. If d is small, the spherical segments may become disconnected; if d is chosen "too large," the overhangs and cavities will be "smoothed over." In either case the construction of $\zeta(x, y)$ from a *single microscopic* configuration does involve an element of the arbitrary: Either the size of the grid or the collision diameter of the probe must be given. On the scale of small k any reasonable choice of d not too different from $d = 1$ will produce the same result. Moreover, with $d = 1$, Eq. (15) was found to be verified within the accuracy of the data. The safest route to unambiguous quantitative information is through the DDCF. Thus we have extracted four structure factors,

$$S_{\alpha\beta}(\mathbf{k}) \equiv \langle \rho_{\mathbf{k}}^{\alpha} \rho^{\beta}{}_{\mathbf{k}} \rangle_{\sigma} \tag{16}$$

for $\mathbf{k} \neq 0$. The limit $\mathbf{k} = 0$ must be treated separately

$$S_{\alpha\beta}(0) = \langle N_\alpha N_\beta \rangle_\sigma - \langle N_\alpha \rangle_\sigma \langle N_\beta \rangle_\sigma \tag{17}$$

The average over box v_σ, $\langle \ldots \rangle_\sigma$ is a grand-canonical average with fixed volume V and variable N_α. The conditions for stability of this subsystem are $S_{\alpha\alpha} > 0$ and Det $\|S\| > 0$.

For $\mathbf{k} = 0$ the fluctuation of $N = N_a + N_b$ in volume v_σ is also positive and related to the compressibility of the subsystem in v_σ; therefore we construct the sum (also for $k \neq 0$)

$$S_{NN} = S_{aa} + S_{ab} + S_{ba} + S_{bb} \qquad (S_{ab} = S_{ba}) \tag{18}$$

We found that all four S's display a $1/k^2$ divergence but S_{NN} displays none. Its weak k dependence is quite like $S(k)$ in bulk [4]. S_{NN} is one of the Bhatia–Thornton structure factors [15, 16] used to convert $S_{\alpha\beta}\,\delta\mu_\alpha\,\delta\mu_\beta$ to a sum of 2 squares [14]. Here μ is the chemical potential. Alternatively, we introduce a linear transformation to $\mu_a + \mu_b$, $-\mu_a + \mu_b$, which produces S_{NN}, S_{Nd}, and $S_{dd} \equiv S_{aa} - 2S_{ab} + S_{bb}$. Both S_{Nd} and S_{dd} diverge as $1/k^2$. The exact diagonalization of the 2×2 matrix $\mathbf{S}$ ensures there will be no

mixed term; of the two eigenvalues λ_1, λ_2, one shows no divergence and the other does. It is practical to consider the inverse matrix $\mathbf{S}^{-1}$ and its eigenvalues $1/\lambda_1$, $1/\lambda_2$; then

$$1/\lambda_2(k) = c_0 + k^2 c_2 + k^4 c_4 + \ldots \tag{19}$$

Quantitative agreement, within the accuracy of our data, was obtained by first interpolating S_{dd} to its value at $k = 0$ and subtracting—thus assuming $S \sim S_{CW} + S_{bulklike}$—to obtain the CW contribution. We find $D = 0$ [cf. Eq. (13)], the coefficient of k^2 equal to $\beta\gamma$ with excellent accuracy, and the (bending) coefficient of k^4 positive. If we interpret the entire CW denominator [cf. Eq. (13)] as $\beta\gamma(k)$, we find $\gamma(k) = \gamma(0) + b_4 k^2 + b_6 k^4 + \ldots$ with $b_4 = +0.38$, $b_6 = +0.04$, all in LJ units. These plots cannot be shown through lack of space but see Fig. 2. Note how the short-distance peak in the bulk near $k^2 = 40$ is broadened and shifted to lower k in the interface. The density in r_σ is much lower than the bulk density ~ 0.8408.

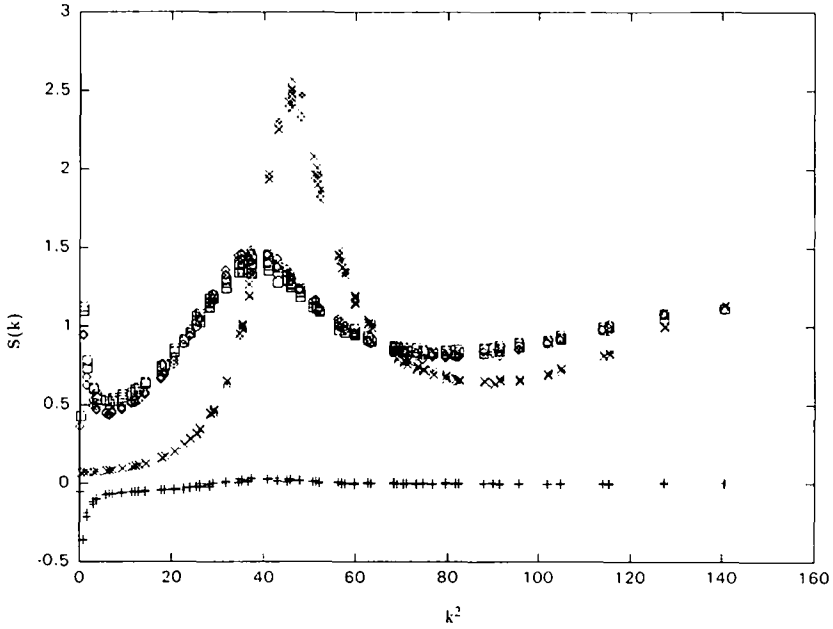

Fig. 2. Structure factors S_{α} as defined by Eqs. (16) and (17) and S_{bulk} determined from a large box in the middle of "a" phase—normalized to allow for a common plot: S_{aa}/N_a (diamonds), $S_{ab}/(N_a + N_b)$ (crosses), S_{bb}/N_b (squares), S_{bulk}/N_{box} (λ's). Here $N_a = 21.87$, $N_b = 17.86$, $N_{box} = 272$. Run of 205,000 timesteps.

5. DENSITY–DENSITY CORRELATIONS $I(k, t)$ and $S(k, \omega)$

The dynamics of fluid surfaces have been studied experimentally by light-scattering and the theory based on macroscopic hydrodynamics has been extensively developed over decades, in its many variants summarized, e.g., by Loudon [17]. He developed i.a. the case of two liquids in contact (also with identical parameters) separated by a thin film (which may be vacuum) [17]. A statistical and hydrodynamic theory of Desai and Grant [18] extended the work of Turski and Langer [19]. In essence the macroscopic theory predicts, for small k and ω, the dispersion relation $\omega^2 \sim k^3$, which is *unobtainable* from the CW theory as we know it; in Ref. 18 it is demonstrated how the latter leads to a k^4 instead of the correct k^3 dependence. There are many reasons for further research either by analytic theory or by simulations: a lack of theory of transport coefficients in the interface, validity of macroscopic hydrodynamics at large k and/or ω, the connection of elastic coefficients introduced by M. Baus [20] with experiment or simulation, etc. There is an early attempt in Ref. 1 but limited to self-diffusion. We are currently studying other transport coefficients by simulation [21]. Loudon [17] discusses the interplay of three functions; $\omega_{\text{cap}}(k) \sim k^{(3/2)}$, damping frequency $\omega_{\text{D}} = \eta k^2/\rho$, and the sound dispersion relation $\omega = ck$. Unfortunately, the simulation window is situated near the two crossings of these three lines. We have made a study of the intermediate scattering function of the interface

$$I_\sigma(k, t) \equiv \langle \rho_{\text{a}}(k, t)\, \rho_{\text{a}}(-k, 0) \rangle_\sigma \tag{20}$$

where

$$\rho_{\text{a}}(k, t) = \sum_{j \in \text{a}}^{N_{\text{a}}} e^{ikr_j(t)} \tag{21}$$

The interfacial box v_σ is defined in Section 4. Then $S_{\text{aa}}(k, \omega)$, abbreviated to $S(k, \omega)$, is defined as

$$S(k, \omega) = 2\text{Re} \int_0^\infty dt e^{i\omega t} I_\sigma(k, t) \tag{22}$$

The autocorrelation function $I(k, t)$ is determined from a sequential record of $\rho_{\text{a}}(k, t)$; the subsequent Fourier transformation is marred by truncation artifacts and statistics, which is never good enough for long times. Due to lack of space we do not show plots of $I_\sigma(k, t)$ and $I_{\text{bulk}}(k, t)$, but generally the initial decay is much slower for I_σ, especially for low values of k. Figure 3 shows a comparison of $S(\omega)/N_{\text{a}}$ with $S_{\text{bulk}}(\omega)/N_{\text{bulk}}$ for a low

value of k^2; for higher values of k^2 the two curves differ much less at all values of ω. Asymptotic decay $\sim\omega^{-4}$ predicted by Desai and Grant [18] has been found, as well as ω^{-2} decay of $S_{\text{bulk}}(\omega)$.

Experimental $S_{\text{bulk}}(k, \omega)$ have been interpolated [22] by a sum of three modes,

$$S \sim \text{Re} \sum_{j=-1}^{+1} A_j(k)/[i\omega + z_j(k)] \tag{23}$$

with $A_0(k)$ and $z_0(k)$ real and $z_{+1} = \text{c.c.}(z_{-1})$. This semiempirical form is compatible with hydrodynamics [22] and *also* with interfacial hydrodynamics of Ref. 18 for a particular choice of the parameters which are in Eq. (23) free functions of k. This expression can be transformed from ω to t variable; under the assumption that the resulting expressions can also be used for short times, these are being used for a direct estimate of the damping coefficient(s).

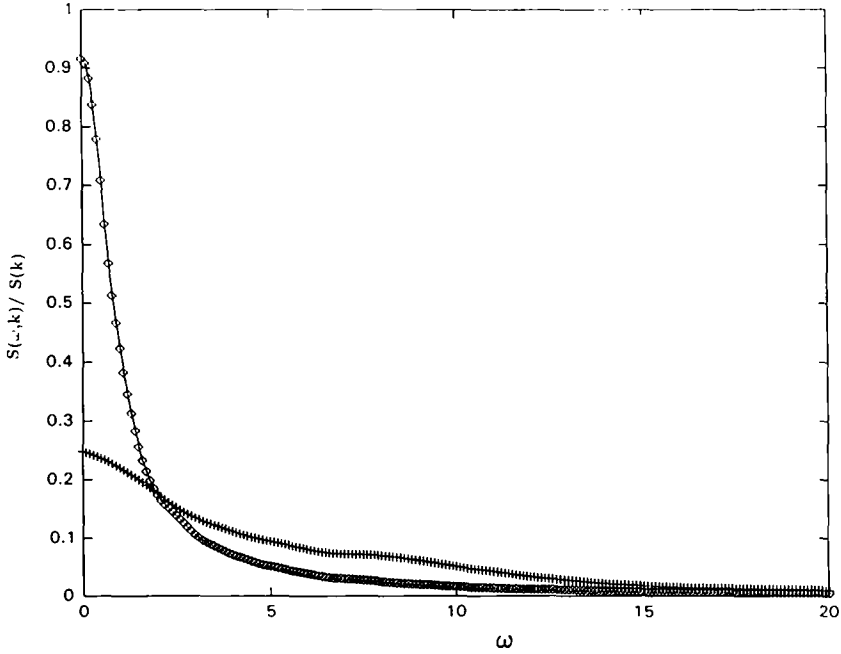

Fig. 3. $S_{aa}(k, \omega)$ normalized to static $S(k)$ compared with the same quantity from the bulk (diamonds and crosses, respectively $k^2 = 2(2\pi)/L_x)^2$.

ACKNOWLEDGMENTS

The author is indebted to Dr. S. Toxværd for numerous discussions and also to Professor R. Evans for a discussion. The work was supported by NATO Sci. Div. (Brussels). He is also indebted to Dr. Toxværd and to the University of Copenhagen for the computer time.

REFERENCES

1. M. Meyer, M. Maréchal, and M. Hayoun, *J. Chem. Phys.* **89**:1067 (1988).
2. J. S. Rowlinson and B. Widom, *Molecular Theory of Capillarity* (Clarendon, Oxford, 1982).
3. R. Evans, in *Les Houches, Session XLVIII, 1988, Liquids at Interfaces* (Elsevier, New York, 1989); see also *Inhomogeneous Fluids*, D. Henderson (Academic Press, New York, 1992), Chap. 1.
4. S. Toxværd and J. Stecki, *J. Chem. Phys.* (in press).
5. R. Evans, J. R. Henderson, D. C. Hoyle, A. O. Parry, and Z. A. Sabeur, *Mol. Phys.* **80**:755 (1993).
6. J. Dudowicz, *J. Phys. A Math. Gen.* **21**:2441 (1988), A. Ciach, J. Dudowicz, and J. Stecki, *Physica A* **145**:327 (1987); *Phys. Rev. Lett.* **56**:1482 (1986).
7. A. Ciah, *Phys. Rev. B* **34**:1932 (1986); A. Ciach and J. Stecki, *J. Phys. A Math. Gen.* **20**:5619 (1987).
8. P. C. Hemmer and B. Lund, *J. Phys. A Math. Gen.* **21**:3463 (1988).
9. J. Stecki and P. C. Hemmer, *J. Phys. A Math. Gen.* **23**:1735 (1990).
10. S. Toxværd, *Mol. Phys.* **72**:159 (1991); *Mol. Phys.* **76**:1397 (1992).
11. H. Goldstein, *Classical Mechanics* (Addison Wesley, Reading, MA, 1952).
12. J. P. Hansen and I. R. McDonald, *Theory of Simple Liquids* (Academic Press, New York, 1990).
13. Usually the factor $1/N$ is included; see Ref. 12.
14. R. Evans and T. J. Sluckin, *J. Phys. C Solid State Phys.* **14**:2569 (1981).
15. A. B. Bhatia and D. E. Thornton, *Phys. Rev. B* **2**:3004 (1970).
16. A. Parola and L. Reatto, *J. Phys. Condensed Matter* **5**:B165 (1993).
17. R. Loudon, in *Surface Excitations*, V. M. Agranovich and A. A. Maradudin, eds. (North-Holland, Amsterdam, 1984), Chap. 6.
18. R. C. Desai and M. Grant, in *Fluid Interfacial Phenomena*, C. A. Croxton, ed. (Wiley, New York, 1986), Chap. 3.
19. L. A. Turski and J. S. Langer, *Phys. Rev. A* **22**:2189 (1980), where references to earlier work can be found.
20. M. Baus, *J. Chem. Phys.* **76**::2003 (1982).
21. P. Padilla, J. Stecki, and S. Toxværd (unpublished).
22. A. A. van Well, P. Verkerk, L. A. de Graaf, J.-B. Suck, and J. D. R. Copley, *Phys. Rev. A* **31**:3391 (1985).